DIRAC NOTE 2013–06

Investigation of systematic errors and estimation of πK atom lifetime

V. Yazkov
Skobeltsyn Institute of Nuclear Physics, Lomonosov Moscow State University, Russia
M. Zhabitsky
Joint Institute for Nuclear Research, Dubna, Russia

November 5, 2013

Abstract

This note describes details of analysis of data sample collected by DIRAC experiment on Ni target in 2008–2010 in order to estimate lifetime of πK atoms. Experimental results consists of six distinct data samples: both charge combinations (π^+K^- and $K^+\pi^-$ atoms) obtained in different experimental conditions corresponding to each year of data-taking. Sources of systematic errors are analyzed, and estimations of systematic errors are presented. Taking into account both statistical and systematic uncertainties, the lifetime of πK atoms is estimated by maximum likelihood method.

1 $P_{\rm br} = P_{\rm br}(\tau)$ from theory

Lifetime of $A_{\pi K}$ in the ground state is related to $a_0^- = \frac{1}{3}\left(a_0^{1/2} - a_0^{3/2}\right)$ scattering length [1]:

$$\frac{1}{\tau} = \Gamma_{\pi K} \approx \Gamma(A_{\pi K} \to \pi^0\overline{K^0}) = \Gamma(A_{K\pi} \to \pi^0 K^0) = 8\alpha^3\mu_+^2 p^*(a_0^-)^2(1+\delta_K), \quad (1)$$

$$\delta_K = (4.0 \pm 2.2) \times 10^{-2}. \quad (2)$$

By using $a_0^- m_{\pi^+} = 0.090 \pm 0.005$ [2] theory estimates πK atom lifetime

$$\tau_{1S}^{\rm th} = (3.5 \pm 0.4) \times 10^{-15} \text{ s}. \quad (3)$$

While propagating through the target foil, relativistic πK atoms can be ionized or get excited due to interaction with target atoms. General formulas for total and excitation cross sections in Born approximation were derived in work [3] for the case of relativistic $\pi^+\pi^-$ atoms. Same authors calculated a set of total and excitation cross sections for projectile πK atoms, which is used in this note. Break-up (ionization) of πK atoms is concurrent to their annihilation. Therefore there is a one-to-one correspondence between the lifetime and the probability for πK atom to break-up $P_{\rm br}$. More generally for a foil of thickness s the probability of break-up is a function of atomic lifetime and momentum p in the laboratory frame: $P_{\rm br} = P_{\rm br}(\tau, p)$. Above function is calculated [4] as a solution of a system of kinetic equations. Ni targets of thickness 98 μm and 108 μm [5] were used by the experiment in 2008 and 2009–2010 respectively.

Distributions $P_{\rm br}(\tau, p)$ integrated over experimental spectra dN/dp (Fig. 2) of reconstructed π^+K^- pairs with low relative moment are presented in Fig. 1. Similar distribution was obtained for $K^+\pi^-$ atoms.

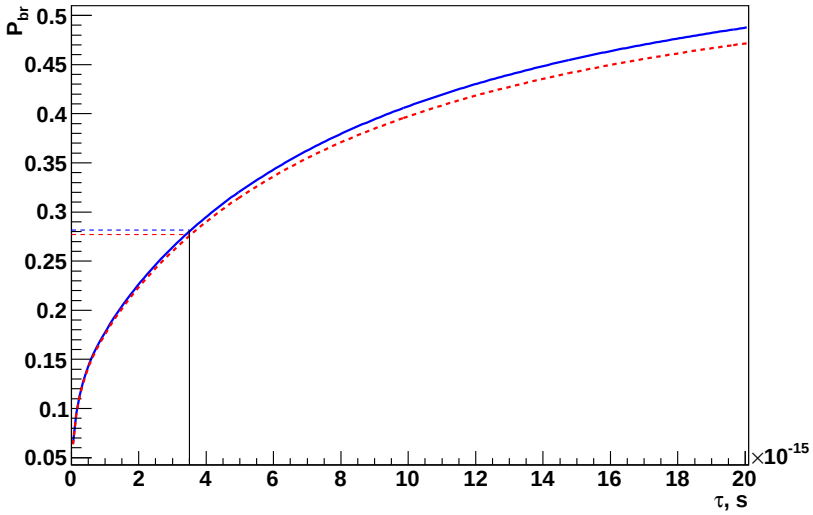

Figure 1: Probability of $A_{\pi K}$ break-up as a function of its lifetime in the ground state in Ni target of thickness 98 μm (dashed) and 108 μm (in 2009) (solid) in the DIRAC experimental conditions

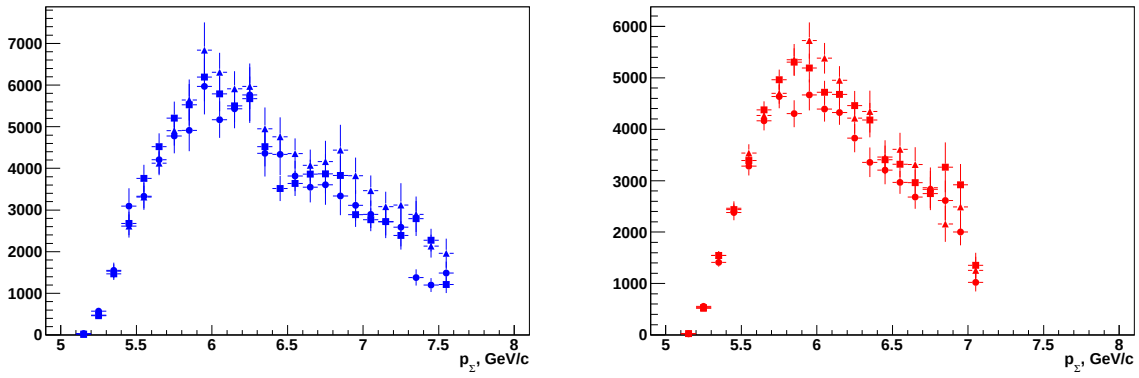

Figure 2: Experimental spectra of π^+K^- (left) and $K^+\pi^-$ (right) pairs for different data periods: 2008 ($\circ$), 2009 (Δ) and 2010 ($\Box$)

2 Experimental data

Experimental values $P_{\rm br}$ from (Q_L, Q_T)- and Q_L-analysis of statistics collected on Ni targets are presented in Tab. 1 and Tab. 2, respectively. Performed analysis follows procedures described in the article [6]. Here we cite only results of fits of experimental distributions. Excessive number of digits is preserved to avoid round-off errors.

Table 1: Experimental $P_{\rm br}$ from (Q_L, Q_T)-analysis and corresponding estimations of πK atom lifetime in the ground state $\hat{\tau}$. Only statistical uncertainties are cited.

Atom	Year	s, μm	$P_{\rm br}$	n_A	$\hat{\tau}$, fs
$A_{\pi K}$	2008	98	0.4117 ± 0.3292	21 ± 13	$11.31^{+\infty}_{-11.21}$
$A_{\pi K}$	2009	108	0.3402 ± 0.2435	26 ± 16	$5.86^{+77.1}_{-5.70}$
$A_{\pi K}$	2010	108	0.5827 ± 0.3548	35 ± 16	$> 2.0 (CL = 0.84)$
$A_{\pi K}$	2008–2010			82 ± 26	$10.94^{+\infty}_{-8.47}$
$A_{K\pi}$	2008	98	0.1077 ± 0.1490	14 ± 19	$0.24^{+2.74}_{-0.24}$
$A_{K\pi}$	2009	108	0.1967 ± 0.1725	33 ± 26	$1.38^{+6.20}_{-1.38}$
$A_{K\pi}$	2010	108	0.2971 ± 0.1913	49 ± 26	$4.20^{+16.55}_{-3.99}$
$A_{K\pi}$	2008–2010			96 ± 41	$1.18^{+2.57}_{-1.05}$
$A_{\pi K} + A_{K\pi}$	2008–2010			178 ± 49	$2.48^{+2.99}_{-1.77}$

Table 2: Experimental $P_{\rm br}$ from Q_L-analysis and corresponding lifetime estimations $\hat{\tau}$

Atom	Year	s, μm	$P_{\rm br}$	n_A	$\hat{\tau}$, fs
$A_{\pi K}$	2008	98	0.7466 ± 0.6164	35 ± 21	$> 0.4 (CL = 0.84)$
$A_{\pi K}$	2009	108	0.3703 ± 0.3720	28 ± 24	$7.44^{+\infty}_{-7.44}$
$A_{\pi K}$	2010	108	-0.0435 ± 0.2626	-4 ± 22	$< 1.8 (CL = 0.84)$
$A_{\pi K}$	2008–2010			60 ± 39	$0.77^{+6.39}_{-0.77}$
$A_{K\pi}$	2008	98	0.2042 ± 0.2597	25 ± 30	$1.59^{+17.36}_{-1.59}$
$A_{K\pi}$	2009	108	0.3554 ± 0.3266	54 ± 42	$6.79^{+\infty}_{-6.79}$
$A_{K\pi}$	2010	108	0.3920 ± 0.3238	61 ± 42	$9.09^{+\infty}_{-9.03}$
$A_{K\pi}$	2008–2010			140 ± 66	$4.42^{+14.78}_{-4.05}$
$A_{\pi K} + A_{K\pi}$	2008–2010			200 ± 77	$2.44^{+5.43}_{-2.20}$

3 Sources of systematic errors

Different sources of systematic errors have been investigated. Most of them are induced by imperfection in simulation of pair distributions: "atomic", "Coulomb", "non-Coulomb" πK pairs and wrongly identified pairs. Difference of shapes of experimental and simulated distributions at fit procedure leads to bias of estimated parameters, including breakup probability.

3.1 Λ correction

The largest systematic error is induced by uncertainty in correction on Λ-width. DIRAC setup detects proton-pion pairs from decay of Λ particles. Width of distribution over effective masses is defined only by resolution of detectors due to very low decay width of the particle. Comparison of widths for experimental and simulated distributions shows that experimental distribution is wider [7]. It means that errors of laboratory momentum reconstruction are underestimated for Monte-Carlo events. It is shown [7], that this effect could be compensated by additional smearing for reconstructed momenta $P^{\rm rec}$ of simulated particles, using equation:

$$P^{\rm smeared} = P^{\rm rec} \cdot (1. + C_f \cdot N(0.,1.))\,, \tag{4}$$

here N(0.,1.) is a normal distribution centered at 0. with unity width parameter, C_f is a coefficient, which is estimated [7] to be:

$$C_f = 0.0007 \pm 0.0004\,. \tag{5}$$

This smearing have been introduced in analysis of Monte-Carlo data. This correction shifts breakup probability by 0.0068 for two-dimensional (Q_T, Q_L) analysis and 0.012 for one-dimensional (Q_L) analysis. Error in estimation of smearing parameter (Eq. 5) induces systematic errors in breakup probability: $\sigma_\Lambda^{\rm syst} = 0.0039$ for two-dimensional analysis (Q_L, Q_T) and $\sigma_\Lambda^{\rm syst} = 0.0071$ for one-dimensional analysis (Q_L).

Error in parameter C_f is a statistical error of dedicated measurement. Therefore it is possible to expect that probability density for $\sigma_\Lambda^{\rm syst}$ has normal distribution.

3.2 Uncertainty of multiple scattering in Nickel target

The next systematic error is induced by uncertainty in the multiple scattering angle inside the Ni target foil. This scattering provides main contribution to smearing of initial distribution of events over Q_T. It is essential for "Coulomb" and "atomic" pair distribution which have sharp peak at $Q = 0$.

A value of average angle of multiple scattering has been measured with an accuracy 1% [8]. Influence of this parameter on possible bias of measured break up probability of $\pi^+\pi^-$ atoms has been investigated in [9]. For $K^+\pi^-$ and π^+K^- atoms influence is expected to be weaker, because a width of initial peak of Coulomb correlation function is wider by a factor ~ 1.6, following a ratio of Bohr momenta of πK and $\pi\pi$ atoms. As result the same variation of Q_T distribution leads to lower effect. Analysis of πK data with simulated distribution of "atomic", "Coulomb" and "non-Coulomb" pairs, simulated with different average angle of multiple scattering in the Nickel target, allows to obtain estimation of the contribution to a systematic error to be $\sigma_{Ni}^{\rm syst} = 0.0032$ for two-dimensional analysis and $\sigma_{Ni}^{\rm syst} = 0.00054$ for one-dimensional analysis.

Error in average angle of multiple scattering in the target is a statistical error of dedicated measurement. Therefore it is possible to expect that probability density for $\sigma_{Ni}^{\rm syst}$ has normal distribution.

3.3 Response of SFD and IH detectors.

Fiber detector (SFD) is used for definition of open angle of pair and provides reconstructed value of pair Q_T. For simulation of SFD response it is needed to take into account resolution of detector, efficiency, two track resolution and probability of background hits [10]. The most problematic fraction of events contains one of particle of pair which does not produce a signal in one of SFD planes. In this case there is probability that tracking procedure takes single hit in proper region of SFD plane as a result of passing this column by a close pair of particles with very small opening angle (defined by detector pitch 0.0205 cm and a base from a target to SFD plane — 300 cm) in this projection. At condition of DIRAC experiment it is possible for pairs which have real distance up to 2 cm. Evidently it provides essential error in Q_T measurement. To decrease fraction of wrongly measured events, Scintillation Ionization hodoscope (IH) is used [11]. Double or single amplitude in corresponded slabs of IH allows to identify close pair from background of single particles. In addition to hits from particle of investigated pair, some background hits could be detected both in SFD and IH detectors. It also affects accuracy of Q_T measurement. To achieve good agreement of experimental and Monte-Carlo data response of SFD detector has been investigated [12]. For IH a set of double-amplitude criteria for experimental data and simulated data have been tuned to provide the same admixture of single particles for events accepted by criterion.

On Fig. 3 there are experimental distributions over difference in X-plane of SFD for different interval of differences in Y-plane (and vice versa) in units of detector pitch. Points with error bars present experimental distribution of $\pi^+\pi^-$, blue line - simulated distribution, red line - simulated distribution after correction. Procedure selects events with $Q_L > 10$ MeV/c. It allows to suppress dependence of Coulomb effect on Q_T and, as result, on ΔX and ΔY. There is peak at distance 0 (both particles hit one column) and 2 deeps for -1 and +1. It is known effect induced by two-particle resolution [10]. But there is peak in range ± 5, which is higher for low values of ΔY (ΔX) and is less for big ΔY (ΔX). Such correlation could be mark of e^+e^- pairs. But background of electron-positron pairs strongly suppressed by Cherenkov and and Preshower detectors. Also simulated $\pi^+\pi^-$ pairs (blue line) reproduce qualitatively this behavior. Most probable explanation is physical background in SFD planes. It could be δ-electron or photon which is produced by pion and hit one neighbors column. If signal from second pion is lost due to inefficiency, tracking procedure could take background signal and to produce artificial close pair. Criterion on double amplitude in IH is not applied in this case, because there are two different hits for 2 tracks.

Existence of strong correlation between X- and Y-projection for experimental data could be explained by background e^+e^- pairs which hit upstream detectors but are not detected by downstream detectors due to too soft (or hard) momentum. Downstream detectors detects particles originated from the same proton-nuclear interaction but through decays of long lived particles like charged kaons. Due to change of track parameters at decay point these tracks are not found by global fit procedure, but could occasionally provide artificial combination with close pair hits in SFD from soft e^+e^- pair. Fraction of such pairs increases after applying of selection criteria $|Q_X| < 6$ MeV/c, $|Q_Y| < 4$ MeV/c.

On Fig. 4 there are distributions over $\delta Q_X = |Q_X^{\rm at}| - |Q_X|$. Here Q_X is reconstructed value of relative momentum projection for simulated pair, $|Q_X^{\rm at}|$ is a value for the same pair on exit of target, known from history of simulated event. Variable $\delta Q_Y = |Q_Y^{\rm at}| - |Q_Y|$ is defined in the same way. There is essential difference between shape of distribution for different combination of ΔX and ΔY which are in phase with analysis of Fig. 3. To achieve good agreement of experimental and simulated distribution a weight of events with $\delta Q_X > 1$ MeV/c or $\delta Q_Y > 1$ MeV/c was increased by a coefficient depended on coordinate difference in X-, Y- and W-planes. Corrected distributions are presented on Fig. 3 by red lines.

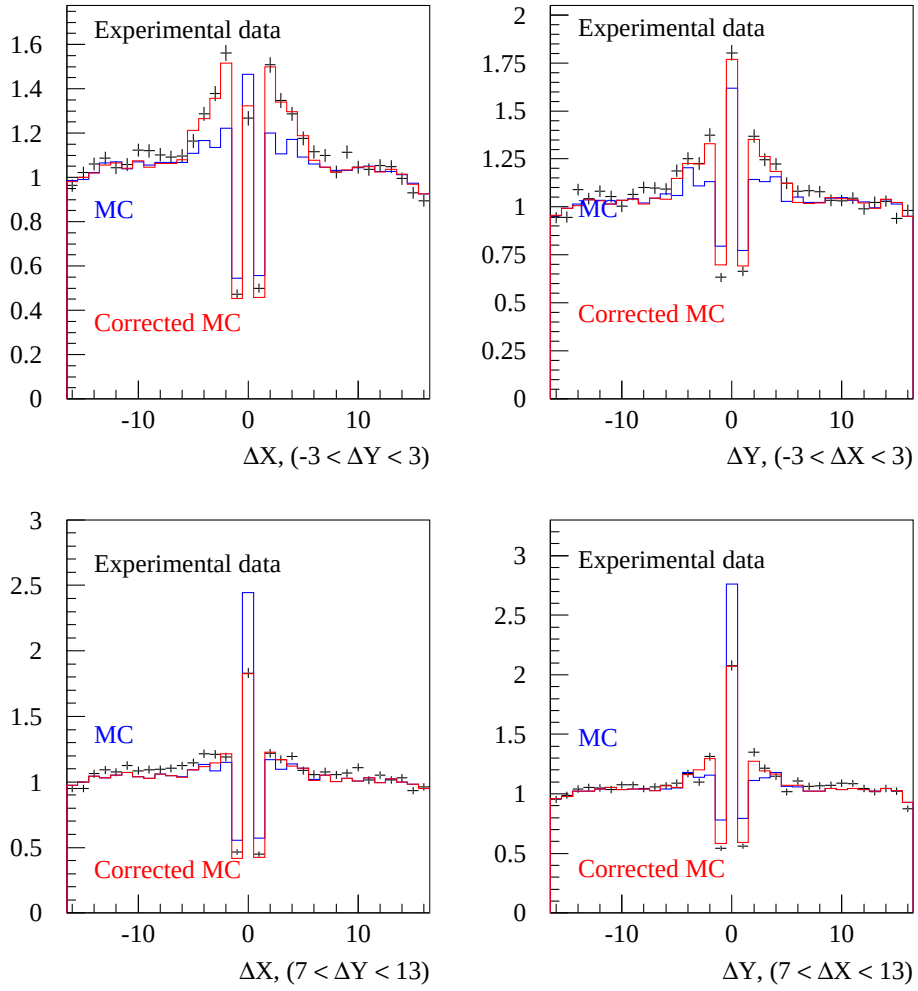

Figure 3: Distributions over ΔX (left) and ΔY (right) in detector pitch units for different ranges of ΔY and ΔX, correspondingly. Experimental data presented by points with error bars, simulated data - blue lines, simulated data after correction - red lines

For estimation of possible error, experimental data have been analysed in two version of simulated events weighting. For one of them procedure takes into account only part of simulated data ($|Q_X|, |Q_Y| < 10$ MeV/c). In another (final) approach procedure takes into account that wrong close pair identification could be up to $|Q_X|, |Q_Y| < 30$ MeV/c. A difference gives a scale of sensitivity of break up probability to these effect. For two-dimensional analysis shift of result is 0.0013 and for one-dimensional analysis it is 0.0005. It is possible to expect that probability density for systematic error is uniform distribution in a range ± 0.0013 (± 0.0005). It provides corresponded values of systematic errors to be: $\sigma^{\rm syst}_{SFD} = 0.0008$ (Q_L, Q_T) and $\sigma^{\rm syst}_{SFD} = 0.0003$ (Q_L).

3.4 Finite size of production region

Correlation function for "Coulomb pair" production is different from standard Gamow-Sommerfeld factor [13, 14, 15, 16]. As result a shape of correlation function depends on fractions of π and K mesons, produced from different sources (direct processes, ρ, ϕ, ω, η'). Data have been analyzed using correlation functions obtained in point-like and finite size production region assumptions.

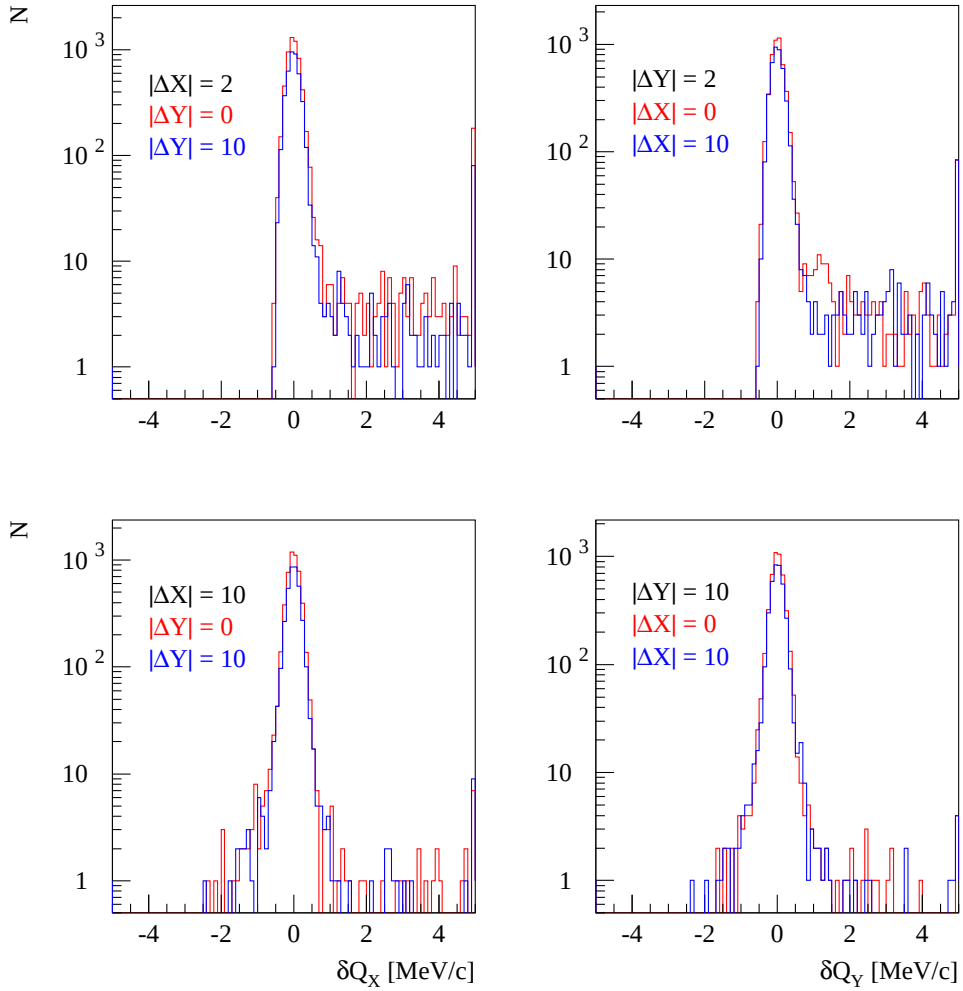

Figure 4: Distributions over ΔQ_X (left) and ΔQ_Y (right) for different ranges of ΔX and ΔY

Breakup probability difference is found to be 0.0002 for one- and two-dimensional analysis. Accuracy of production region size description depends on accuracy of knowledge about fraction of different sources at production of π and K mesons. We could suppose that their accuracy is at least not worse than estimated value. It is assumed that density of probability for this contribution to systematic error is uniformly distributed in a range from 0.5 to 1.5 of shifted value. Therefore systematic error estimation is $\sigma_{fsz}^{\text{syst}} = 0.00006$.

3.5 Accuracy of measurement for laboratory momentum spectra of πK and background pairs

All systematic errors mentioned above have the same values for $K^+\pi^-$ and π^+K^- collected in 2008, 2009 and 2010 runs. The next two systematic errors are induced by uncertainty in measurement of spectra πK and background. These spectra have been measured individually for different run periods and produce systematic errors in P_{br}: $\sigma_{\pi K}^{\text{syst}}$ and $\sigma_{\text{backgr}}^{\text{syst}}$ which are independent for different data sets.

Background of electron-positron pairs is suppressed by nitrogen Cherenkov counter (ChN) at first level of trigger. But there is some admixture of e^+e^- pairs due to big flux of such pairs

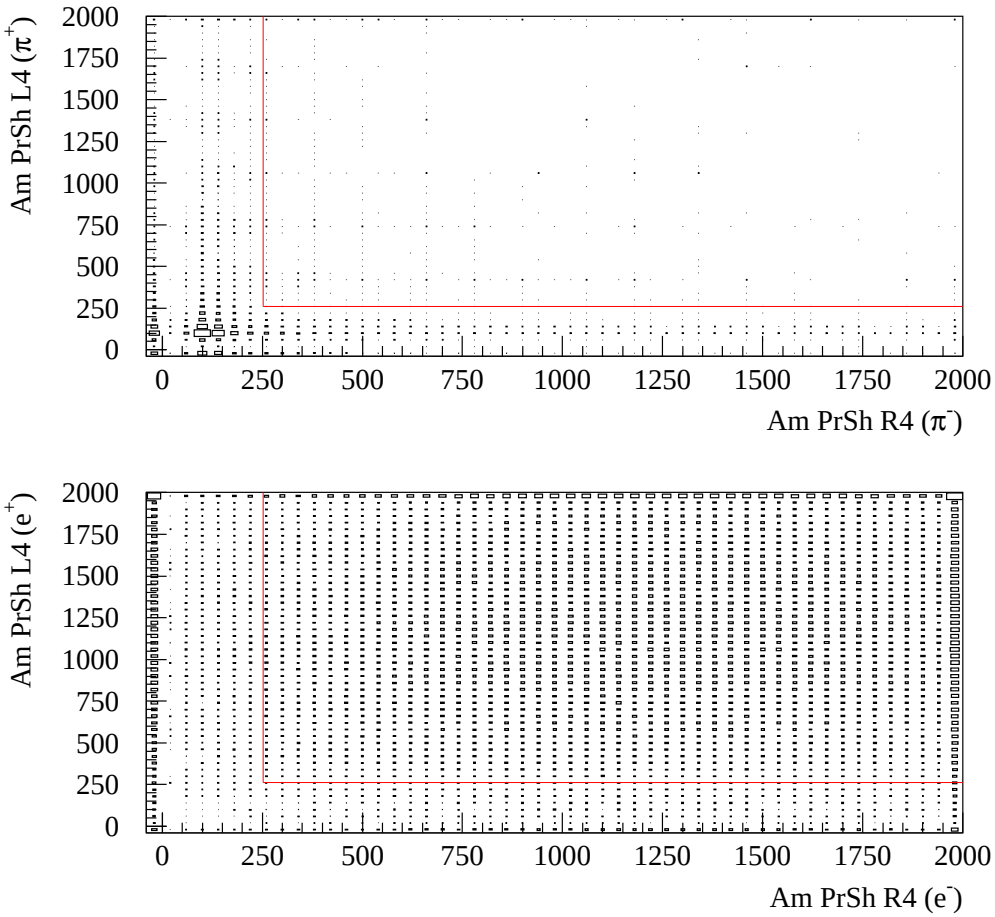

Figure 5: Upper: distribution over amplitudes of Preshower for negative (along X-axis) and positive (along Y-axis) hadrons. Lower: distribution for amplitudes of e^- (along X-axis) and e^+ (along Y-axis). e^+e^- pairs on lower picture

with small Q_T (due to specific features of e^+e^- pair production) and finite ChN efficiency. For additional suppression Preshower scintillation detector is used. Distribution of $\pi^+\pi^-$ (hadron) pairs over amplitudes of Preshower for negative (along X-axis) and positive (along Y-axis) is shown on Fig. 5 (upper picture). Similar distribution for e^+e^- pair is shown on Fig. 5 (lower picture). It is seen that distributions are different which allows to implement criterion on amplitude shown by red line. Also it is possible to find fraction of e^+e^- pairs is accepted by this criterion.

Result of this criterion is shown on Fig. 6 for e^+e^- and $\pi^+\pi^-$ (hadron) pairs. Black line is initial distribution over Q_T for events with signals in ChN (e^+e^-) and without signals in ChN (hadrons). Red line shows events after applying criterion on Preshower amplitudes. On the next step rejected events were subtracted from distributions with weight which describe ratio of non-rejected and rejected events. Final distributions are shown by magenta line. It is seen that this procedure strongly suppresses e^+e^- with losses 2.5% of hadron pairs. Systematic error due to admixture of e^+e^- pairs is assumed to be negligible.

Due to finite efficiency of detectors some admixtures of $\pi^+\pi^-$, $\mathrm{p}\pi^-$ and $\pi^+\bar{\mathrm{p}}$ pairs present

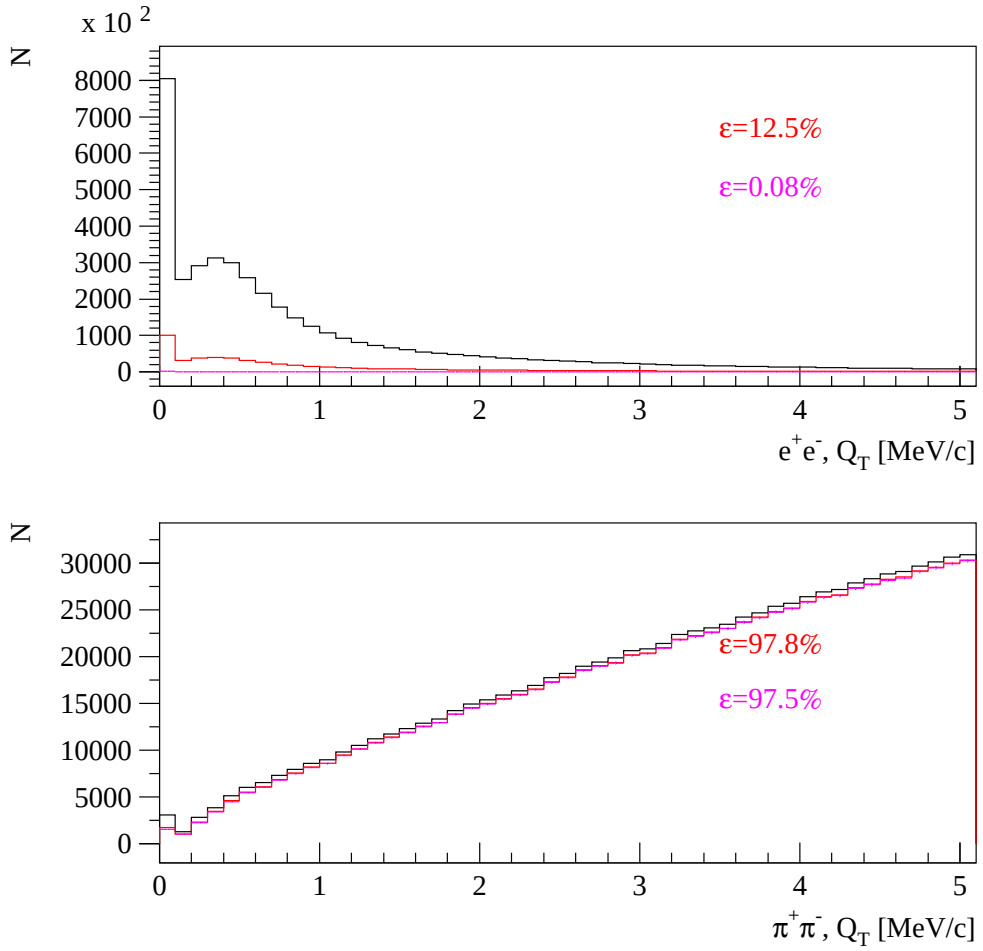

Figure 6: Upper: distributions over Q_T for e^+e^- pairs before and after criterion on amplitudes of Preshower. Lower: similar distributions for $\pi^+\pi^-$ (hadron) pairs before and after criterion on amplitudes of Preshower

in final experimental distribution. Also there is background of "accidental pairs" generated in different proton-nuclear interaction. All these pairs have different distribution over difference (ΔT) of generation time for positive and negative particles. Experimental distribution over ΔT is presented on Fig. 7 for $K^+\pi^-$ pairs collected in 2008 with momentum of positive particle in a range $4.5 < P < 4.6$ GeV/c, under assumption that a positive particle is K^+ and a negative one — π^-. Here criterion on ΔT is not applied. On Fig. 8 similar distributions are presented for π^+K^- pairs.

This analysis allows to obtain fractions of useful events and background as function of K meson momentum. On Fig. 9 there are distributions over laboratory momentum of positive particles for $K^+\pi^-$ (red), $\pi^+\pi^-$ (blue) and pπ^- (magenta) pairs collected in 2008-2010. Distribution for π^+K^- (red), $\pi^+\pi^-$ (blue) and $\pi^+\bar{\text{p}}$ (magenta) pairs over laboratory momentum of negative particle are presented in Fig. 10.

Background of "accidental pairs" could be subtracted, because it is possible to estimate amount of such pairs under signal peak (see Fig. 8) and to subtract distribution of accidental pairs collected in outside region, using coefficient which takes into account ratio of "accidental pair" number under a peak to number of "accidental pairs" in outside region.

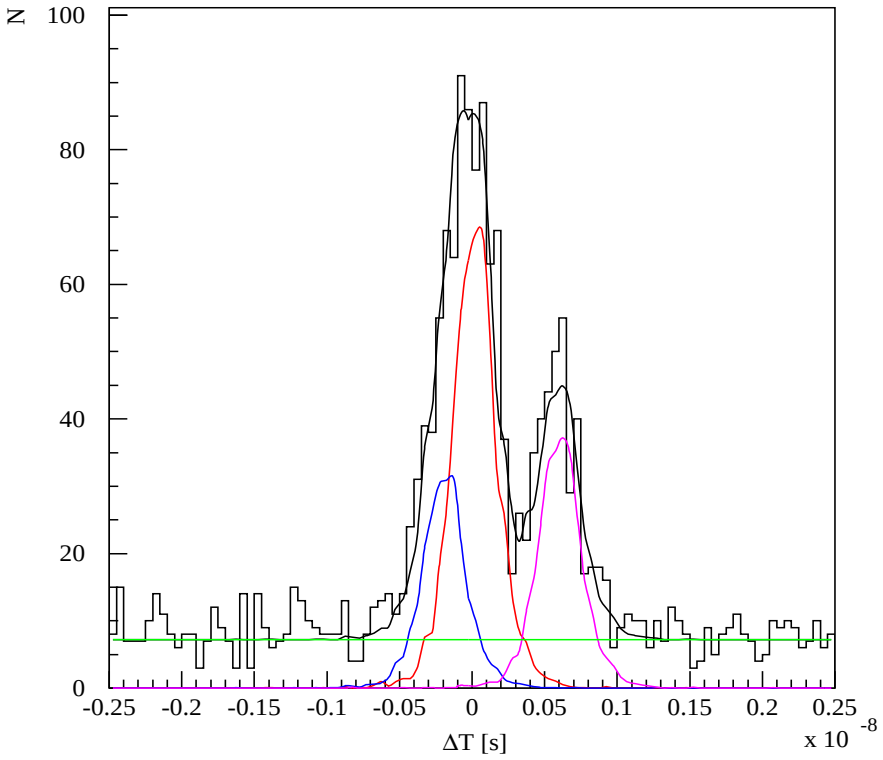

Figure 7: Distribution over $K^+\pi^-$ pairs difference of particle generation times with momentum of positive particle in a range $4.5 < P < 4.6$ GeV/c. $K^+\pi^-$ pairs shown by red, $\pi^+\pi^-$ pairs are blue, pπ^- pairs are magenta, "accidental pairs" are green

Background of non-identified $\pi^+\pi^-$, pπ^- and $\pi^+\bar{\text{p}}$ has been simulated with Monte-Carlo "non-Coulomb pairs", because for ratio of laboratory momenta of π and K mesons, which provides small relative momenta Q for πK pair, relative momentum Q for $\pi^+\pi^-$ and pπ^- pairs is very big and Coulomb factor is close to 1. Laboratory momentum spectrum of simulated "non-Coulomb" πK pairs has been modified to correspond to a spectrum of background pairs (a sum of $\pi^+\pi^-$, pπ^- from Fig. 9, or a sum of $\pi^+\pi^-$ and $\pi^+\bar{\text{p}}$ from Fig. 10). On Fig. 11 simulated distribution of "Coulomb" (blue), "non-Coulomb" (magenta) and background (black) pairs over Q_L (with criterion $Q_T < 4$ MeV/c) are presented. Distributions are normalized to have value 1 in the last bin. It is seen that shape of "Coulomb pair" distribution has peak at low Q due to Coulomb interaction in the final state. Distribution of background pairs also has additional slope relative to a distribution of "non-Coulomb" pairs. It is induced by different distribution over laboratory momentum, which provides different limitation of particle momentum difference by the DIRAC setup acceptance. As result, presence of background particles leads to overestimation of "Coulomb pair" fraction by a fit procedure, and following to underestimation of "atomic pair" number and breakup probability value. To prevent this, simulated distribution of background pairs is subtracted from experimental distribution.

But spectrum of background is measured with final accuracy. Therefore uncertainty of spectrum leads to a systematic error in breakup probability. To describe uncertainty program simulates alternative version of laboratory momentum spectrum of background particles. Value of i-th bin is modified as:

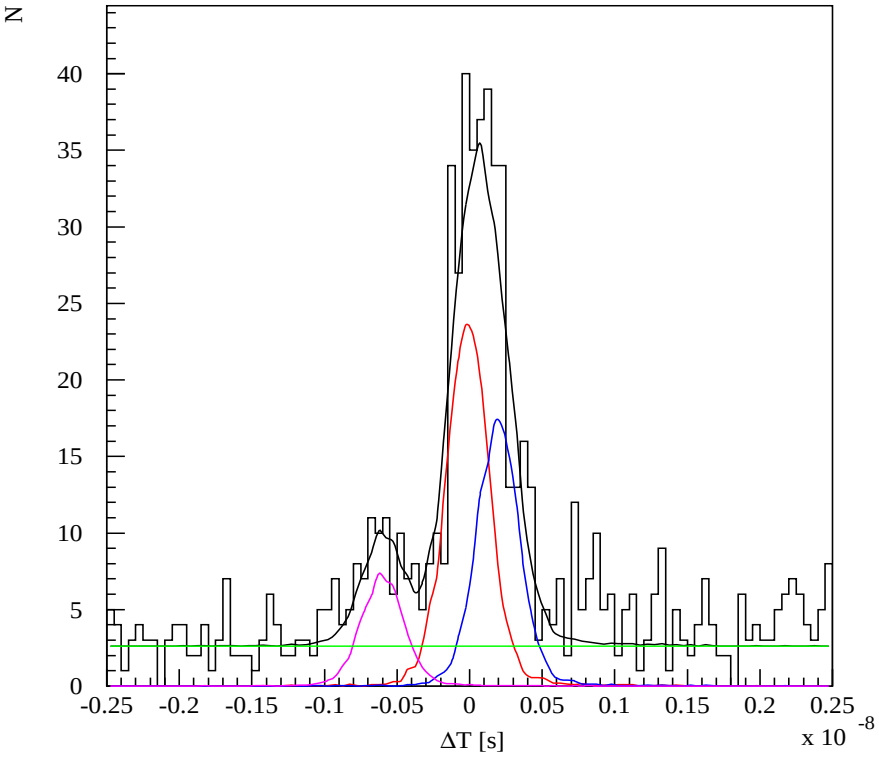

Figure 8: Distribution over π^+K^- pairs difference of particle generation times with momentum of negative particle in a range $4.5 < P < 4.6$ GeV/c. π^+K^- pairs shown by red, $\pi^+\pi^-$ pairs are blue, $\pi^+\bar{\text{p}}$ pairs are magenta, "accidental pairs" are green

$$F^{'}(P_i) = F(P_i) + E(P_i) \cdot N(0., 1.)\,. \tag{6}$$

Here $F(P_i)$ is a measured value in i-th bin, $E(P_i)$ — statistical error of measured value and $F^{'}(P_i)$ is modified value. Ratio of modified distribution to initial one has been fitted by a linear function:

$$\frac{F^{'}(P_i)}{F(P_i)} = p_0 \cdot (1 + p_1 \cdot (P_i - P^*))\,. \tag{7}$$

Here p_0 and p_1 are free parameters of fit, P^* is a fixed parameter which is chosen to provide zero correlation between p_0 and p_1. Finally fit procedure gives estimation of errors for p_0 and p_1. This estimation represents accuracies of total amount of background pairs and of slope of momentum distribution. Varying fraction of background and slope of its distribution, procedure provides shifts of breakup probability. Because correlation between p_0 and p_1 is defined to be 0, these biases are summed as two independent random values and provide an estimation for $\sigma^{\text{syst}}_{\text{backgr}}$.

Similar analysis has been performed for accuracy of πK spectrum measurement. But in this case only error in slope of distribution is a source of systematic error. Bias of breakup probability is taken as an estimation for $\sigma^{\text{syst}}_{\pi K}$.

Estimations for these to kinds of systematic errors are shown in Table 3 for different data sets.

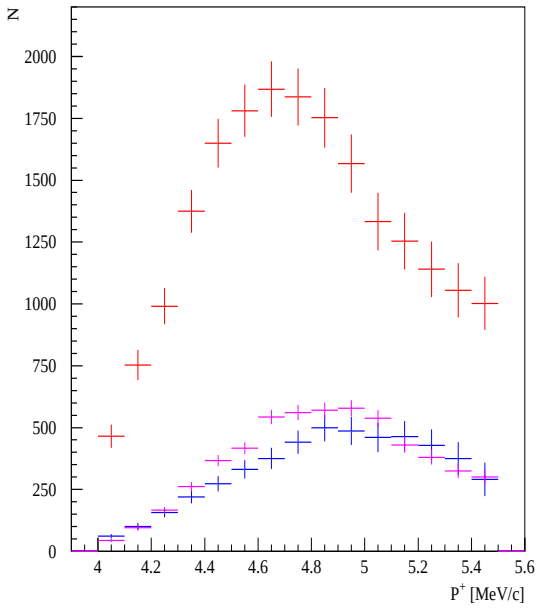

Figure 9: Distributions of $K^+\pi^-$ (red), $\pi^+\pi^-$ (blue) and $p\pi^-$ (magenta) pairs over laboratory momentum of positive particle

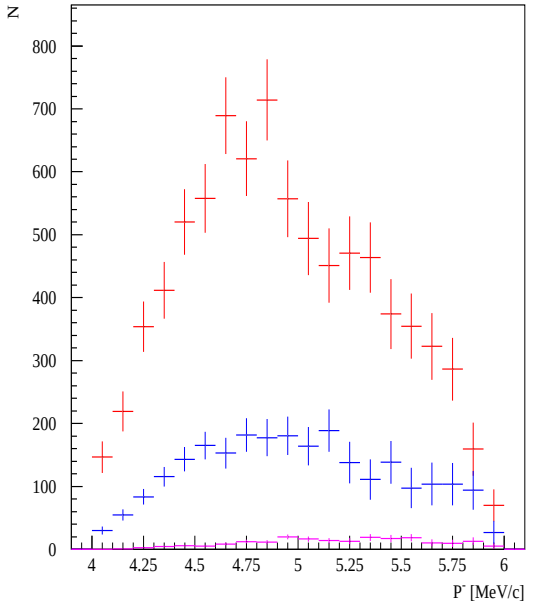

Figure 10: Distributions of π^+K^- (red), $\pi^+\pi^-$ (blue) and $\pi^+\bar{p}$ (magenta) pairs over laboratory momentum of negative particle

3.6 Uncertainty in $P_{\rm br}(\tau)$ relation

Through the thorough calculations of total and excitation cross sections of relativistic $\pi^+\pi^-$ atoms with Ni atoms, it was shown that $P_{\rm br}(\tau)$ dependence calculated in first Born approximation is

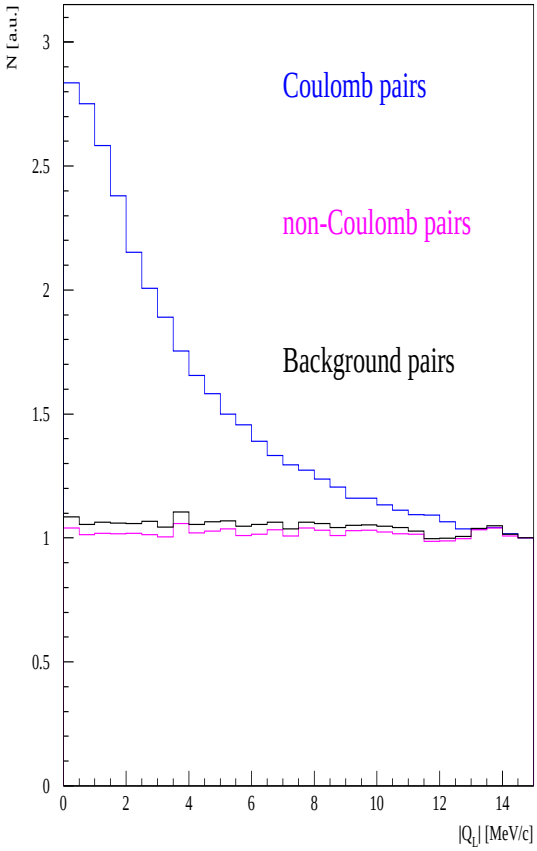

Figure 11: Simulated distributions of "Coulomb" (blue), "non-Coulomb" (magenta) and background (black) pairs over Q_L with criterion $Q_T < 4$ MeV/c

Table 3: Systematic uncertainties in $P_{\rm br}$ due to accuracy of measurement of πK laboratory spectra and background pairs

Year	$\sigma^{\rm syst}_{\pi K}$	$\sigma^{\rm syst}_{\rm backgr}$
$K^+\pi^-$ over Q_T, Q_L		
2008	0.0028	0.0015
2009	0.0044	0.0025
2010	0.0036	0.0022
$K^+\pi^-$ over Q_L		
2008	0.0030	0.0028
2009	0.0053	0.0044
2010	0.0046	0.0036
π^+K^- over Q_T, Q_L		
2008	0.0072	0.0067
2009	0.0048	0.0028
2010	0.0017	0.0043
π^+K^- over Q_L		
2008	0.0093	0.0072
2009	0.0047	0.0048
2010	0.0021	0.0017

shifted by about 3% [17] with respect to more precise approaches. Due to higher reduced mass of πK atoms, they are even more compact with respect to pionium, therefore we should expect that in their case the corresponding relation is known with better precision. In this work we have used cross sections in first Born approximation to calculate $P_{\rm br}(\tau)$ dependence. We approximate this contribution by a uniform distribution in the range $P_{\rm br} \times (1, 1.03)$. We do not shift the central value of $P_{\rm br}$. Corresponding systematic uncertainty is $\sigma_{cs}^{\rm syst} = 0.005$, which is correlated for all data periods and atomic charge combinations.

Target thickness was measured with precision better than $\pm 1\,\mu$m [5]. This corresponds to $\sigma_s^{\rm syst} = 3 \cdot 10^{-4}$ in $P_{\rm br}$ relation, which can be safely neglected.

Another source of uncertainties is a precision of πK spectra dN/dp (Figs. 9, 10) used for convolution with $P_{\rm br}(\tau, p)$ into $P_{\rm br}(\tau)$. To estimate systematic uncertainty due to limited statistical precision of dN/dp spectra. we performed a series of N statistical tests. For each test a distribution dN/dp was modified: independent random values, generated according to the Normal distribution $N(0, \sigma)$ with a width corresponding to a bin's uncertainty, were added to content of each bin. This resulted in a series of $P_{{\rm br},i}(\tau)$ dependencies. After sorting a systematic uncertainty was estimated as a half-difference between $[0.84N]$th and $[0.16N]$th $P_{{\rm br},i}$ values. Corresponding systematic error is $2 \cdot 10^{-4}$. It is independent between different samples.

All values of systematic errors have been used for procedure of πK atom lifetime estimation described below.

4 Analysis with systematic errors

Estimations of lifetime in the ground state have been performed by maximum likelihood method according to [18]:

$$L(\tau) = \exp\left(-U^T G^{-1} U/2\right), \tag{8}$$

where $U_i = m_i - P_{\mathrm{br},i}(\tau)$ is a vector of differences between measured values of break-up m_i (Tab. 1) and corresponding theoretical functions $P_{\mathrm{br},i}(\tau)$ for a data sample i. G is the error matrix on U, which includes both statistical σ_i and systematic uncertainties:

$$G_{ij} = \delta_{ij}\left(\sigma_i^2 + (\sigma_i^{\mathrm{syst}})^2\right) + (\sigma_{\mathrm{global}}^{\mathrm{syst}})^2. \tag{9}$$

Where

$$(\sigma_i^{\mathrm{syst}})^2 = (\sigma_{\pi K,i}^{\mathrm{syst}})^2 + (\sigma_{\mathrm{backgr},i}^{\mathrm{syst}})^2, \tag{10}$$

$$(\sigma_{\mathrm{global}}^{\mathrm{syst}})^2 = (\sigma_{\Lambda}^{\mathrm{syst}})^2 + (\sigma_{Ni}^{\mathrm{syst}})^2 + (\sigma_{SFD}^{\mathrm{syst}})^2 + (\sigma_{fsz}^{\mathrm{syst}})^2 + (\sigma_{cs}^{\mathrm{syst}})^2 + (\sigma_{s}^{\mathrm{syst}})^2. \tag{11}$$

The systematic uncertainties σ_i^{syst} are expected to be uncorrelated between different data samples.

If one combines both charge combinations ($A_{\pi K}$ and $A_{K\pi}$) and uses all statistics collected in 2008–2010, then (Q_L, Q_T)-analysis leads to following estimation of the lifetime in the ground state

$$\hat{\tau} = 2.48^{+2.99}_{-1.77}\big|_{\mathrm{stat}}\ ^{+0.30}_{-0.13}\big|_{\mathrm{syst}}\ \mathrm{fs} = 2.48^{+3.01}_{-1.77}\big|_{\mathrm{tot}}\ \mathrm{fs} = 2.5^{+3.0}_{-1.8}\ \mathrm{fs}. \tag{12}$$

Here total uncertainties correspond to the analysis with both statistical and systematic errors, while to estimate statistic uncertainties in the lifetime, systematic errors have been omitted. Systematic uncertainty in the lifetime estimation is defined through the following expression

$$(\sigma_\tau^{\mathrm{syst}})^2 = (\sigma_\tau^{\mathrm{tot}})^2 - (\sigma_\tau^{\mathrm{stat}})^2. \tag{13}$$

Likelihood functions with corresponding confidence levels are shown in Fig. 12. For commodity, all likelihood functions were normalized in a way that their maxima are at the same value: $\max L(\tau) = 1$.

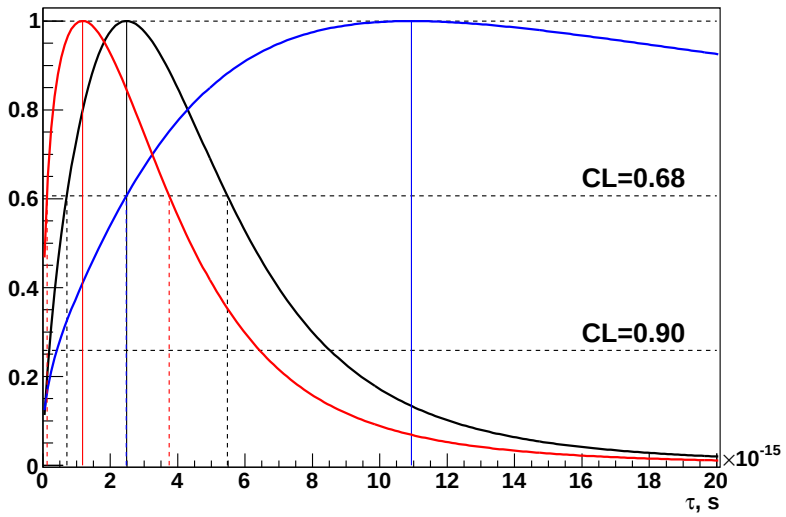

Figure 12: Likelihood functions for $A_{\pi K}$ (blue), $A_{K\pi}$ (red) and combined (black) lifetime estimations. (Q_L, Q_T)-analysis

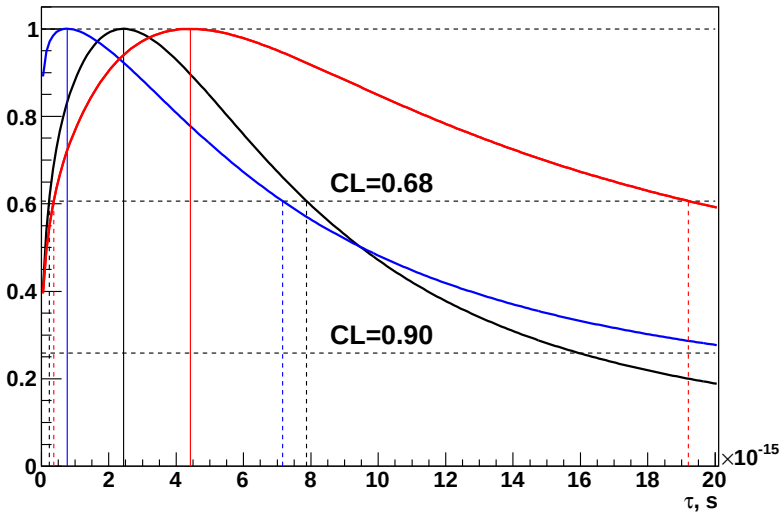

Figure 13: Likelihood functions for $A_{\pi K}$ (blue), $A_{K\pi}$ (red) and combined (black) lifetime estimations. Q_L-analysis

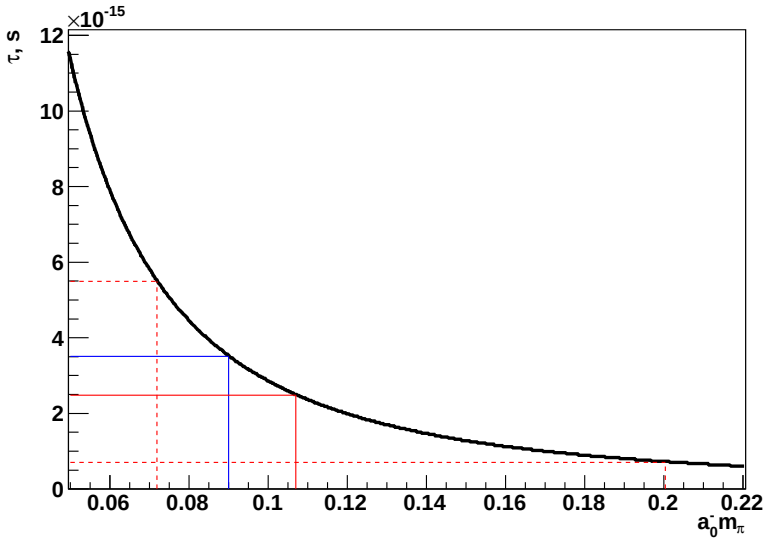

Figure 14: Dependence of $A_{\pi K}$ lifetime in the ground state τ_{1S} on a_0^-. Experimental result from Tab. 1 (red) vs theoretical estimation Eq. (3) (blue). (Q_L, Q_T)-analysis.

Similar estimation of lifetimes has been calculated within Q_L-analysis (Tab. 2).

$$\hat{\tau} = 2.44^{+5.43}_{-2.20}\big|_{\rm stat}\ ^{+0.45}_{-0.07}\big|_{\rm syst}\ {\rm fs} = 2.44^{+5.45}_{-2.21}\big|_{\rm tot}\ {\rm fs} = 2.4^{+5.5}_{-2.2}\ {\rm fs}. \tag{14}$$

Likelihood functions with corresponding confidence levels are shown in Fig. 13.

Lifetime in the ground state estimation (12) from (Q_L, Q_T)-analysis corresponds to πK scattering length a_0^- according to Eq. (1)

$$\left|a_0^-\right| m_{\pi^+} = 0.11^{+0.09}_{-0.04}. \tag{15}$$

To estimate maximal effect from possible linear correlations between systematic uncertainties for different periods, we will treat $\sigma^{\rm syst}_{\pi K,i}$ as they are linearly correlated for a chosen charge-

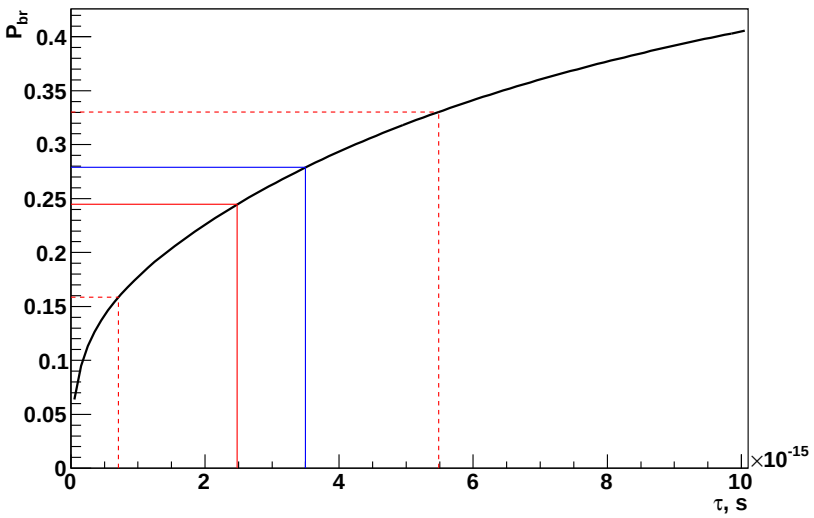

Figure 15: Experimental result Eq. (12) (red) and theoretical estimation Eq. (3) (blue) are superimposed over $P_{\rm br}^{\rm eff}(\tau)$ dependence. (Q_L, Q_T)-analysis.

combination (either π^+K^- or $K^+\pi^-$):

$$\sigma^{\rm syst}_{\pi K,ij} = \sqrt{\sigma^{\rm syst}_{\pi K,i}\sigma^{\rm syst}_{\pi K,j}}. \tag{16}$$

At the same time similar linear correlation is introduced for systematic uncertainties due to background admixtures $\sigma^{\rm syst}_{\rm backgr}$. Then overall result from (Q_L, Qt)-analysis reads:

$$\hat{\tau} = 2.48^{+2.99}_{-1.77}\big|_{\rm stat}\ ^{+0.33}_{-0.15}\big|_{\rm syst}\ {\rm fs} = 2.48^{+3.01}_{-1.77}\big|_{\rm tot}\ {\rm fs}. \tag{17}$$

Thus possible correlations between data samples due to specific systematic errors will not modify final result in a significant way due to smallness of systematic uncertainties in comparison to statistical errors.

There is no direct way to calculate final $P_{\rm br}$ from measurements of $P_{\rm br}$ on different targets and in different experimental conditions (Tab. 1). Just for a presentation one can estimate «effective» $P_{\rm br}$ by projecting $\hat{\tau}$ from Eq. (12) using an effective $P_{\rm br}^{\rm eff}(\tau)$ dependence, e.g.

$$P_{\rm br}^{\rm eff}(\tau) = \frac{\sum n_{A,i} P_{{\rm br},i}(\tau)}{\sum n_{A,i}}, \tag{18}$$

where $n_{A,i}$ is a number of atomic pairs reconstructed for a data sample i. Corresponding effective probability of break-up reads

$$P_{\rm br}^{\rm eff} = 0.24 \pm 0.09. \tag{19}$$

One should note, that this effective value will be different if one selects another $P_{\rm br}^{\rm eff}(\tau)$ dependence or changes cuts in analysis.

References

[1] J. Schweizer, Decay widths and energy shifts of $\pi\pi$ and πK atoms. Phys. Lett. B. 2004. V. 587. PP. 33–40.

[2] P. Büttiker, S. Descotes-Genon and B. Moussallam, A new analysis of πK scattering lengths from Roy and Steiner type equations. Eur. Phys. J. C 2004. V. 33. PP. 409–432.

[3] L.G. Afanasyev and A.V. Tarasov, Phys. Atom. Nucl. 1996. V. 59. P. 2130.

[4] M. Zhabitsky, Direct calculation of the probability of pionium ionization in the target, Phys. At. Nucl. **71**, No. 6, 1040 (2008); arXiv:0710.4416 [hep-ph].

[5] A. Dudarev, M. Nikitin, Measurement of scatterers thickness. DIRAC Note 2012–09, http://cds.cern.ch/record/1526913.

[6] B. Adeva, et al., Determination of $\pi\pi$ scattering lengths from measurement of $\pi^+\pi^-$ atom lifetime, Phys. Lett. B **704**, 24–29 (2011).

[7] A. Benelli, V. Yazkov, Setup tuning using Lambda and anti-Lambda particles, DIRAC-NOTE-2013-03, http://cds.cern.ch/record/1622175.

[8] A. Dudarev et al., Pion multiple Coulomb scattering in the DIRAC experiment (updated version), DIRAC-NOTE-2008-06, http://cds.cern.ch/record/1369639.

[9] V. Yazkov, Investigation of systematic errors for analysis with DC and ScFi, DIRAC-NOTE-2008-04, http://cds.cern.ch/record/1369641.

[10] A. Gorin et al., High resolution scintillating-fibre hodoscope and its readout using peak-sensing algorithm, *NIM*, **A566** (2006) 500.

[11] G. Bitsadze et al., The ionisation hodoscope of the DIRAC experiment, *NIM*, **A533** (2004) 353.

[12] A. Benelli, SFD study and simulation for the data 2008-2010, Talk at DIRAC Collaboration meeting, 26 September 2011, Geneva, Switzerland, DIRAC-TALK-2011-01, http://dirac.web.cern.ch/DIRAC/talks.html

[13] R. Lednicky, Finite-size effect on two-particle production, *J. Phys. G: Nucl. Part. Phys.* **35** (2008) 125109.

[14] P.V. Chliapnikov and V.M. Ronjin, Finite-size correction to the pionium lifetime due to ω and $\eta^{'}$ contributions, *J. Phys. G: Nucl. Part. Phys.* **36** (2009) 105004.

[15] R. Lednicky, On the separation r^*- distribution for pion-kaon pairs in the experiment DIRAC, DIRAC-NOTE-2012-05, http://cds.cern.ch/record/1475781.

[16] P.V. Chliapnikov, Dimesoatoms and correlation functions in two-body inclusive reactions, DIRAC-NOTE-2012-08, http://cds.cern.ch/record/1526911.

[17] C. Santamarina, et al. A Monte Carlo calculation of the pionium break-up probability with different sets of pionium target cross sections, J. Phys. B 36 (2003) 4273–4287.

[18] D. Drijard and M. Zhabitsky, How to extract the lifetime of pionium and $|a_0^0 - a_0^2|$ from the measurements of the pionium ionization probability. DIRAC Note 2008–07, http://cds.cern.ch/record/1367888.